The intermittency of precipitation and the MJO

8B.7

Da Yang* and Andrew P. Ingersoll
Division of Geological and Planetary Sciences
California Institute of Technology
Pasadena, California

1. Introduction:

The Madden-Julian Oscillation (MJO) is an intense rainfall and associated wind pattern in the tropical atmosphere. The MJO can last for 30-90 days, and it propagates eastward slowly (~ 5 m/s) (*Madden and Julian*, 1972, 1994). Both its persistency and slow drift rate are longstanding mysteries in tropical meteorology (Zhang, 2005).

There are two distinct schools of MJO theories. One school considers the MJO as a moisture mode, a large-scale, low-frequency unstable mode in the tropics. The moisture mode arises from positive feedbacks between convection and the source of moist static energy (MSE) (*e.g.*, *Neelin and Yu*, 1994; *Sobel et al.*, 2001; *Fuchs and Raymond*, 2002, 2005, 2007; *Bretherton et al.*, 2005; *Maloney*, 2009; *Raymond and Fuchs*, 2009). Part of the evidence comes from the fact that making deep convection sensitive to free troposphere moisture improves the MJO simulations in general circulation models (GCMs) (e.g., *Grabowski*, 2003; *Bechtold et al.*, 2008; *Holloway et al.*, 2013). Recent studies investigate the MSE budget of the MJO and show that cloud-radiation feedback is the leading component of the MSE budget (e.g., Anderson and Kuang, 2012; Arnold et al., 2013). Horizontal advection of moisture are important to the eastward propagation (e.g., Anderson and Kuang, 2012).

The other school considers the MJO as a large-scale, long-lasting envelope of small-scale high-frequency waves and convection is a set of intermittent and energetic events that are triggered when a certain threshold in the environment is exceeded. *Yang and Ingersoll* (2013, 2014, hereafter YI13 and YI14) suggest that the intermittency of precipitation is key to simulating the MJO. YI13 develop a 2D shallow water model of the MJO that emphasizes the role of triggered convection and high-frequency waves. Convection is parameterized as a short-duration localized mass source and is triggered when the layer thickness falls below a critical value. Radiation is parameterized as a steady uniform mass sink. Over a wide range of parameters, they observed MJO-like signals with the observed drift rate and horizontal strucutres. Based on their simulation results, YI13 propose that the MJO could be an interference pattern of the westward and eastward (WIG and EIG) inertia gravity waves. The propagation speed of the MJO is approximately equal to one-half the phase speed difference between the EIG and WIG waves.

* Corresponding author: Da Yang, Caltech, Pasadena, CA 91125, Email: dyang@caltech.edu

Yang and Ingersoll (2014, hereafter YI14) present a novel 1D β-plane model that successfully simulates the MJO using the same governing mechanism as in YI13 model. Using this 1D model, they derive a scaling theory for the MJO horizontal wavenumber under radiative-convective equilibrium (RCE). This scaling theory says that the MJO wavenumber increases with the number density of precipitation events, and decreases with the Kelvin wave speed.

In addition to the above theoretical studies, there is also growing observational evidence suggesting that the intermittency of precipitation and high-frequency waves might be important to the MJO. *Zuluaga and Houze* (2013) suggest that rainfall is intermittent and separated by non-rainy days during active phases of the MJO. They further propose that the rainfall intermittency is due to high-frequency equatorial waves, which form the large-scale MJO envelope.

In this paper, we will use a 3D GCM to further test if the intermittency of precipitation and high-frequency waves are important to the MJO. In section 2, we describe our GCM and experiment setup. In section 3, we show our simulation results. In section 4, we present our conclusions, discussions, and plans for future work.

2. Model and experiment setup:

We use a 3D moist GCM similar to those described by *O'Gorman and Schneider* (2008), and *Frierson* (2007). This GCM is based on the Geophysical Fluid Dynamics Laboratory (GFDL) spectral dynamical core and has a slab ocean as the lower boundary condition. This GCM uses a gray radiation scheme and a simplified Betts-Miller convection scheme. This convection scheme relaxes temperature and moisture to reference temperature and moisture profiles, which are calculated by assuming a pseudoadiabatic process with a fixed relative humidity. In the original setting, deep convection will happen when both the convective available potential energy (CAPE) and the column water excess (δq) are positive with respect to the reference moisture profile.

To test our hypothesis, we make precipitation more intermittent through raising the deep convection threshold. One way is to raise the CAPE threshold, i.e., convection only happens when CAPE > $CAPE_o$ (hereafter, CAPE experiment). Another way is to raise the δq threshold, i.e., convection only happens when $\delta q > \delta q_o$, (hereafter, δq experiment). The other way is to add a convective inhibition (CIN) criterion. CIN represents the minimum amount of energy to activate convection. In this experiment, convection only happens when CIN < CIN_o (hereafter, CIN experiment). Each of the above methods can make precipitation more intermittent, and we will implement them separately. In this study, we carry out simulations with uniform short wave incoming radiation and uniform optical depth over the globe. This heavily reduces the meridional temperature gradient and therefore reduces the meridional moisture gradient.

3. Simulation results:

Figure 1 shows the Hovmoller diagram of precipitation. In the control experiment (Fig. 1a), we see both eastward and westward propagating equatorial waves, The eastward propagating wave is the Kelvin wave or high frequency EIG wave, and the speed is ~ 20 m/s. The westward propagating wave is the Rossby wave, and the speed is ~ 6 m/s. The MJO is absent in this experiment. Figures 1b, c and d show simulation results from δq, CAPE, and CIN experiments respectively. In all these simulations, there are strong slowly eastward propagating signals, which are the MJOs. The zonal wavenumber of the MJOs ranges from wavenumber 1 to wavenumber 3, and the propagation speeds range from 2.3 m/s to 3.9 m/s. In these MJO envelopes, there are small-scale structures, but the fast propagating Kelvin wave signals are not prominent.

Figure 2 shows the power spectra of the symmetric components of precipitation averaged over 10°S to 10°N in wavenumber and frequency domain. These power spectra are consistent with Fig. 1. Equatorial Rossby and Kelvin waves are present in the control simulation (Fig. 2a), whereas there is no MJO signal in the low-frequency and low positive wavenumber region. In the other three experiments, the MJO signals are strong in the power spectra but the equatorial wave signals are weak.

The MJO signals show similar vertical structures in all three experiments. Figure 3 shows the vertical structure of the MJO composite in the CAPE experiment. Arrows represent vector winds and colors show the specific humidity anomalies associated with the MJO. The composites shown here are based on a common linear regression method (Anderson and Kuang 2012). We filter the MJO precipitation signal in the wavenumber frequency domain and transfer it back to the physical domain. Then we get the MJO composite in precipitation and use the precipitation time series at 180° longitude as the reference time series in regressing other fields. There is low-level wind convergence and upper level wind divergence associated with the MJO convective center. This is consistent with the observed MJO, which shows the first baroclinic structure in wind (Kiladis et al. 2005). The specific humidity leads the MJO convection and shows a significant tilting structure with height.

We have simulated realistic MJOs in δq, CAPE, and CIN experiments, in which we raise the threshold for convection and increase the intermittency of precipitation. We want to further test our hypothesis and examine if these simulations have stronger high-frequency waves compared to the control simulation, in which there is no MJO signal. Figure 4 shows the power spectra with MJO signals normalized by the control simulation power spectrum in the 10-base logarithm scale. Warm colors represent positive values and cold colors represent negative values. The MJO region shows small positive value. The Rossby waves are weaker in the simulations with MJOs. This suggests that Rossby wave dynamics are not essential to the MJO. In contrast, the high-frequency waves are significantly enhanced in the simulation with MJOs. This may suggest that better representation of high-frequency waves helps to improve the MJO simulation.

4. Conclusion and discussions:

In this paper, we carry out GCM simulations with uniformly distributed gray radiation. We have simulated MJO signals through raising the convection threshold in three different ways. Our results suggest that the cloud-radiation feedback and meridional moisture gradient are not essential to the existence and propagation of the MJO. We find that the high-frequency waves are much stronger in the simulation with MJOs. This is consistent with the hypothesis in YI13 and YI14 and suggests that high-frequency waves are important to the MJO.

Previous studies have shown that making deep convection more sensitive to free troposphere relative humidity improves the MJO simulations in GCMs (e.g., *Bechtold et al.*, 2008). They further conclude that the MJO is a moisture mode. In this study, we find that making convection more sensitive to CAPE and CIN can also improve MJO simulations. The common feature of these different convection criteria is to make the precipitation more intermittent and vigorous. Our study therefore suggests that the role of the convection-moisture feedback is to produce intermittent and vigorous precipitation, which in turn excites high-frequency waves that form the large-scale, low-frequency MJO envelope.

We will further study the relation between the high-frequency waves and the MJO in our simulations. We would also like to simulate the MJO in a wide range of

climates. This allows us to explore the MJO dynamics in a wide parameter space and test the scaling theory in YI13.

Reference:

Andersen, J. A., and Z. Kuang (2012), Moist static energy budget of MJO-like disturbances in the atmosphere of a zonally symmetric aquaplanet, *J. Climate*, *25*, 2782–2804.

Arnold, N. P., Z. Kuang, and E. Tziperman (2013), Enhanced MJO-like Variability at High SST, *J. Climate*, *26*, 988–1001.

Bechtold, P., M. Kohler, T. Jung, F. Doblas-Reyes, M. Leutbecher, M. J. Rodwell, F. Vitart, and G. Balsamo (2008), Advances in simulating atmospheric variability with the ECMWF model: From synoptic to decadal time scales, Q. J. R. Meteorol. Soc., 134, 1337–1351.

Bretherton, C. S., P. N. Blossey, and M. Khairoutdinov (2005), An energy-balance analysis of deep convective self-aggregation above uniform SST, *J. Atmos. Sci.*, *62*, 4273–4292.

Fuchs, Z., and D. J. Raymond (2002), Large-scale modes of a nonrotating atmosphere with water vapor and cloud–radiation feedbacks, *J. Atmos. Sci.*, *59*, 1669–1679.

——, and —— (2005), Large-scale modes in a rotating atmosphere with radiative–convective instability and WISHE, *J. Atmos. Sci.*, *62*, 4084–4094.

——, and —— (2007), A simple, vertically resolved model of tropical disturbances with a humidity closure, *Tellus*, *59A*, 344–354.

Holloway, C. E., S. J. Woolnough, and G. M. S. Lister (2012), Precipitation distributions for explicit versus parametrized convection in a large-domain high-resolution tropical case study, *Quart. J. Roy. Meteor. Soc.*, *138*, 1692–1708.

Kiladis, G. N., K. H. Straub, P. T. Haertel (2005), Zonal and Vertical Structure of the Madden–Julian Oscillation, *J. Atmos. Sci.*, **62**, 2790–2809.

Madden, R. A., and P. R. Julian (1972), Description of global-scale circulation cells in the tropics with a 40–50 day period. *J. Atmos. Sci.*, *29*, 1109–1123.

——, and —— (1994), Observations of the 40–50-day tropical oscillation—A review, *Mon. Wea. Rev.*, *122*, 814–837.

Maloney, E. D. (2009), The moist static energy budget of a com- posite tropical intraseasonal oscillation in a climate model, *J. Climate*, *22*, 711–729.

Neelin, J. D., and J.-Y. Yu (1994), Modes of tropical variability under convective adjustment and the Madden–Julian oscillation. Part I: Analytical theory, *J. Atmos. Sci.*, *51*, 1876–1894.

Raymond, D. J., and Z. Fuchs (2009), Moisture modes and the Madden–Julian oscillation, *J. Climate*, *22*, 3031–3046.

Sobel, A. H., J. Nilsson, and L. M. Polvani (2001), The weak temperature gradient approximation and balanced tropical moisture waves, *J. Atmos. Sci.*, *58*, 3650–3665.

Yang, D., Andrew P. Ingersoll (2013), Triggered Convection, Gravity Waves, and the MJO: A Shallow-Water Model, *J. Atmos. Sci.*, *70*, 2476–2486.

Yang, D., and A. P. Ingersoll (2014), A theory of the MJO horizontal scale, Geophys. Res. Lett., 41, doi:10.1002/2013GL058542.

Zhang, C. *(*2005*),* Madden-Julian Oscillation*, Rev. Geophys., 43, RG2003.*

Figures:

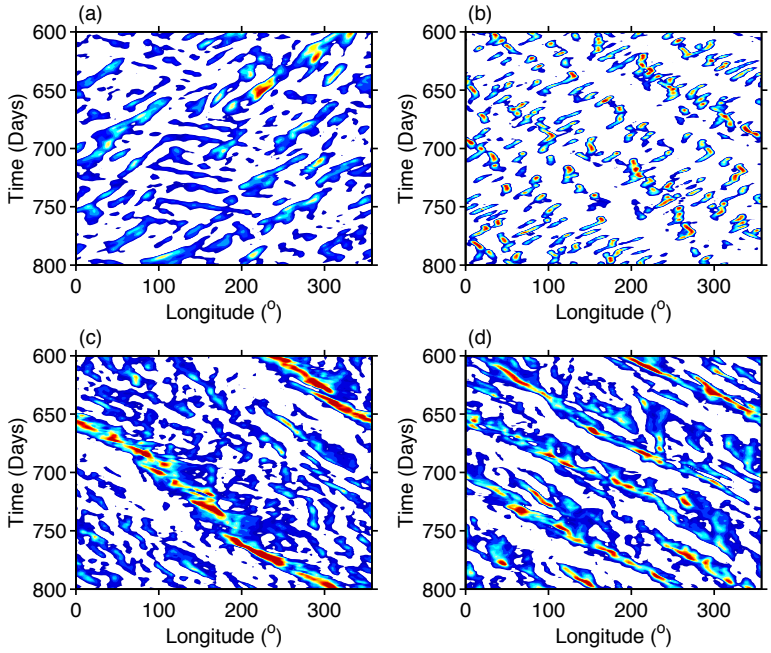

Figure 1. Hovmoller diagram of precipitation averaged over 10°S to 10°N. (a) Control experiment, (b) δq experiment, (c) CAPE experiment, (d) CIN experiment.

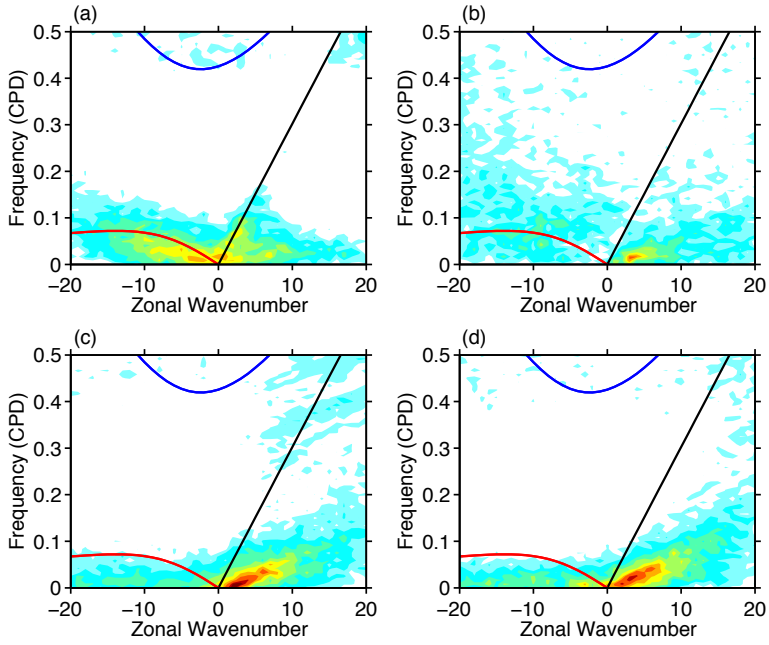

Figure 2. Power spectra of the symmetric component of precipitation averaged over 10°S to 10°N. Background spectra have been removed. (a) Control experiment, (b) δq experiment, (c) CAPE experiment, (d) CIN experiment.

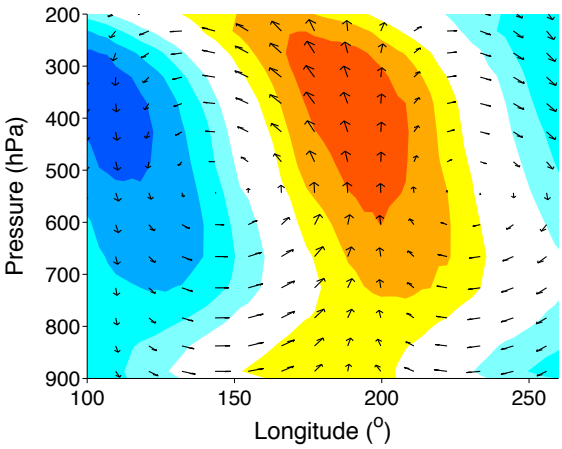

Figure 3. The vertical structure of the MJO composite. Vectors represent the MJO wind anomalies and colors represent the MJO specific humidity anomaly.

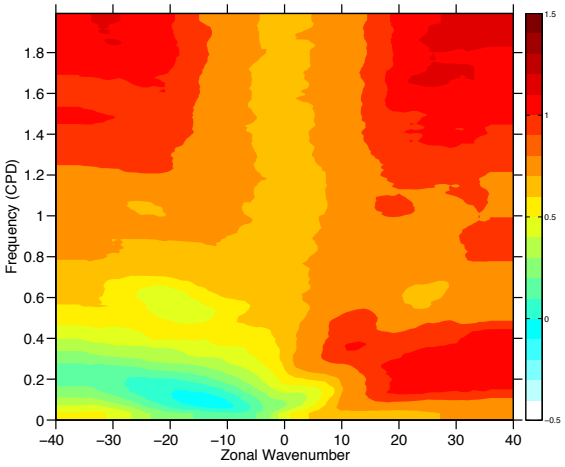

Figure 4. Power spectrum of the CAPE experiment normalized by the control simulation in 10-based logarithm scale.